GL01785

JOURNAL OF GEOPHYSICAL RESEARCH, VOL. 87, NO. B4, PAGES 2815–2828, APRIL 10, 1982

Interpretation of Shallow Electrical Features From Electromagnetic and Magnetotelluric Surveys at Mount Hood, Oregon

N. E. GOLDSTEIN

Earth Sciences Division, Lawrence Berkeley Laboratory, University of California, Berkeley, California 94720

E. MOZLEY

Materials Sciences and Mineral Engineering, College of Engineering University of California, Berkeley, California 94720

M. WILT

Earth Sciences Division, Lawrence Berkeley Laboratory, University of California, Berkeley, California 94720

A magnetotelluric survey, with a reference magnetometer for noise cancellation, was conducted at accessible locations around Mount Hood, Oregon. Thirty-eight tensor magnetotelluric (MT) and remote telluric stations were set up in clusters around the volcano except for the northwest quadrant, a wilderness area. Because of limited access, station locations were restricted to elevations below 1829 m, or no closer than 5 km from the 3424-m summit. On the basis of the MT results, three areas were later investigated in more detail using a large-moment, controlled-source electromagnetic (EM) system developed at Lawrence Berkeley Laboratory and the University of California at Berkeley. One-dimensional interpretations of EM and MT data on the northeast flank of the mountain near the Cloud Cap eruptive center and on the south flank near Timberline Lodge show a similar subsurface resistivity pattern: a resistive surface layer 400–700 m thick, underlain by a conductive layer with variable thickness and resistivity of <20 ohm m. It is speculated that the surface layer consists of volcanics partially saturated with cold meteoric water. The underlying conductive zone is presumed to be volcanics saturated with water heated within the region of the central conduit and, possibly, at the Cloud Cap side vent. This hypothesis is supported by the existence of warm springs at the base of the mountain, most notably Swim Warm Springs on the south flank, and by several geothermal test wells, one of which penetrates the conductor south of Timberline Lodge. The MT data typically gave a shallower depth to the conductive zone than did the EM data. This is attributed, in part, to the error inherent in one-dimensional MT interpretations of geologically or topographically complex areas. On the other hand, MT was better for resolving the thickness of the conductive layer and deeper structure. The MT data show evidence for a moderately conductive north-south structure on the south flank below the Timberline Lodge and for a broad zone of late Tertiary intrusives concealed on the southeast flank.

INTRODUCTION

As part of a geothermal energy assessment of Mount Hood, Oregon, the U.S. Department of Energy (DOE), the U.S. Geological Survey, the U.S. Forest Service, and the State of Oregon's Department of Geology and Mineral Industries have undertaken a series of geological, geochemical, and geophysical studies around this Holocene stratovolcano located 100 km east of Portland, Oregon (Figure 1). Under contract to the U.S. Department of Energy's Division of Geothermal Energy, Lawrence Berkeley Laboratory (LBL) was responsible for geochemical and electrical resistivity surveys [*Goldstein et al.*, 1978; *Goldstein and Mozley*, 1978; *Wilt et al.*, 1979; *Wollenberg et al.*, 1979]. These and other studies were conducted to obtain basic information on the geothermal potential of the area.

Because of the rugged terrain, a general lack of access roads around Mount Hood, and high contact resistance, we concluded early that conventional dc resistivity surveys would be impractical for deep exploration. We therefore embarked on a program of magnetotellurics with a reference magnetometer for noise cancellation and satellite telluric stations [*Goldstein and Mozley*, 1978]. This work, done under contract by Geonomics, Inc., was followed by a controlled-source electromagnetic sounding program in 1978 using the large-moment, EM-60 system [*Morrison et al.*, 1978], developed at LBL and and University of California at Berkeley.

In this paper, we discuss the results of these surveys, comparing the magnetotelluric (MT) and electromagnetic (EM) interpretations and examining the usefulness of these techniques for geothermal prospecting at a High Cascade volcano.

GEOLOGICAL SETTING

Mount Hood is one of several major Pleistocene composite andesitic volcanoes in a chain extending from northern California to British Columbia (Figure 1). Volcanism along this belt is believed by many to result from the eastward subduction of the Juan de Fuca plate beneath the North American plate.

Mount Hood rises some 2500 m above the platform of upper Miocene Columbia River basalts (CRB) and younger Pliocene volcanics consisting of andesitic plugs and flows (Figure 2). Development of the main body of the cone was completed about 20,000 years ago [*Wise*, 1968], and renewed volcanism has occurred at various times since. Several

Paper number 1B1903.

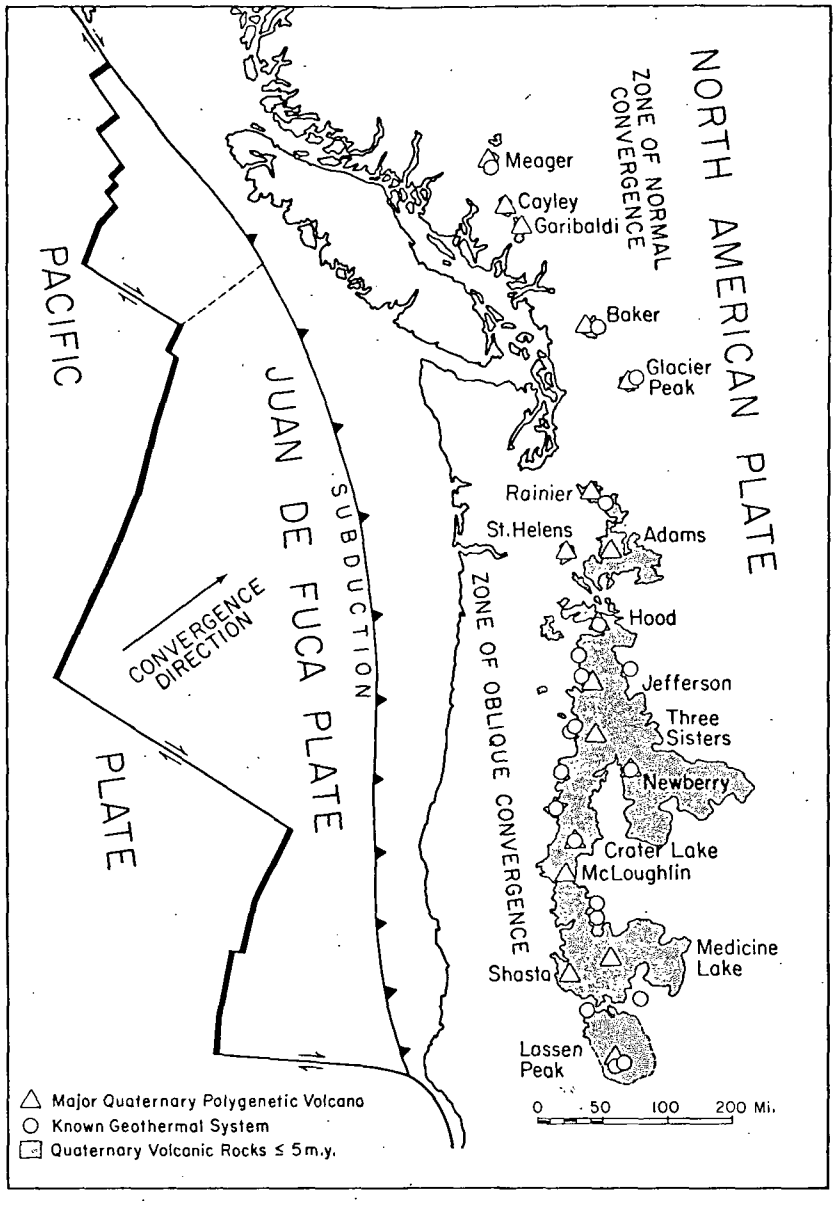

Fig. 1. Location of volcanoes and Holocene volcanic rocks of the Cascade Range [after *Bacon*, 1981].

domes were extruded near the summit about 12,000 years ago [*Crandell and Rubin*, 1977], and later episodes of volcanism caused collapse of the south rim of the crater roughly 1600 years ago. Minor eruptions are reported to have occurred as recently as 1859 and 1865 [*Folsom*, 1970].

Present-day thermal manifestations are warm water springs (Swim Warm Springs), near Summit Meadows on the South flank, and a number of fumaroles in the summit area around Crater Rock, a hornblende dacite plug extruded 200 to 300 years ago [*Crandell*, 1980].

The predominant surficial material covering Mount Hood is andesitic clastic debris. The extensive lava flows predating the debris are mainly hornblende andesite; the more recent extrusions from satellite vents on the north and northeast flanks of the volcano are olivine basalt and olivine andesite. Glacial deposits from the Fraser glaciation period (8000 to 15,000 years ago) and recent mudflows and alluvium fill many of the valleys.

Little substantiated structural information was available when we began the geophysical surveys. *Allen* [1966] stated that Mount Hood lies within a graben formed by the north-south Hood River–Green Ridge faults (along the East Fork of the Hood River) on the east and by unnamed faults recognized by *Thayer* [1937] and *Callaghan* [1933] on the west. On the basis of their gravity survey, *Couch and Gemperle* [1979] concluded that Mount Hood is superimposed on a gravity low that could be a north-south grabenlike structure.

Recently, *Beeson and Moran* [1979] provided new information on a stratigraphic-structural model for the pre-Mount Hood volcanics. They found evidence that the CRB underlying Mount Hood may total 500 m in thickness and have been gently folded into asymmetrical anticlines and synclines striking N40° to 65°E. Some anticlines are thrust-faulted on the northwest limb with thrusting SE to NW. Superimposed on this is a system of NNW trending fractures and faults. Some faults display slickensides, indicating right-lateral movement. The CRB dip gently away from the axis of the High Cascades near Mount Hood, forming a broad structural high that *Beeson and Moran* [1979] postulate to be a consequence of crustal swelling caused by intrusion.

Before this study there were few reported electrical stud-

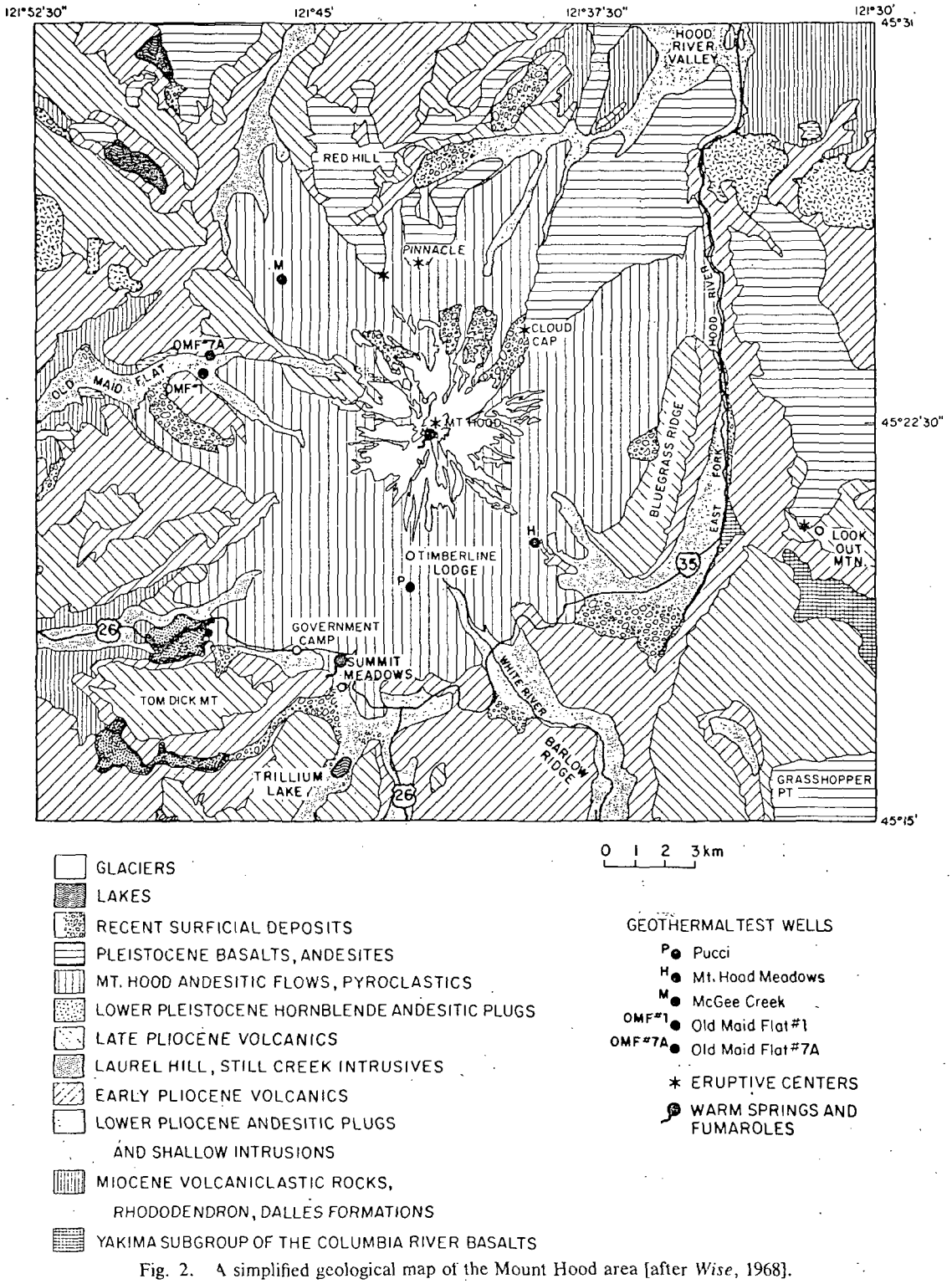

Fig. 2. A simplified geological map of the Mount Hood area [after *Wise*, 1968].

ies of the crust beneath the Cascades and no studies specific to any one of the Quaternary volcanoes. *Law et al.* [1980] made deep geomagnetic depth soundings at six stations in an east-west line crossing the Cascades 120 km north of Mount Hood—the line passing between Mount Rainier and Mount St. Helens. They found evidence for a north-south conductivity anomaly close to the axis of the High Cascades, and they fitted the anomaly to a line current at a depth of 17 km. Because of nonuniqueness, the source might also correspond to a current system up to 50 km wide located at a shallower depth. They also found evidence in the quadrature component for a near-surface conductor. The U.S. Geological Survey [*Stanley*, 1982] later contracted for a regional MT survey at widely spaced lines across the Cascades, with one line at roughly the same latitude as the geomagnetic sounding stations. Because of poor data quality or three-dimensional effects in the data, no detailed interpretation was done. The MT electrical strike, however, has a N70°E trend, which *Stanley* [1980] shows is parallel to the strike of a large gravity low (–100 mGal) crossing the Cascades obliquely between the Columbia River and Mount Rainier. The MT data indicate a conductor to the south or toward the gravity

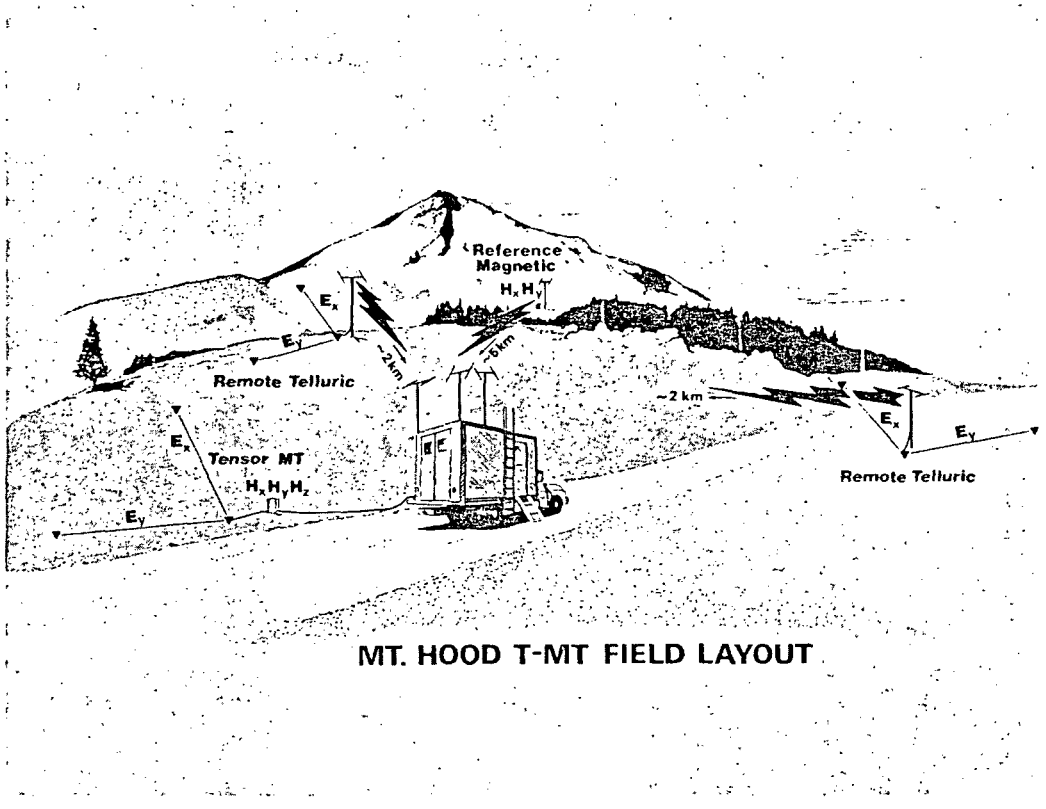

Fig. 3. A schematic diagram of the telluric-magnetotelluric data acquisition method with a reference magnetometer.

low. Thus, from these two limited surveys, one might argue for both a crustal conductor oriented north-south beneath the Cascades and a large, near-surface block of less dense, but relatively conductive, Holocene volcanics north of the Columbia River.

GEOPHYSICAL SURVEY INSTRUMENTATION AND PROCEDURES

Magnetotelluric Surveys

Magnetotelluric surveys were performed in two phases by Geonomics, Inc., from June to November 1977. Each setup consisted of a tensor MT base station plus two remote telluric stations and one remote magnetic station at distances of 2–4 km from the base station (Figure 3). From each remote site, electrical and magnetic field data were telemetered via an FM radio link to the base station, where all data, in three overlapping bands from 0.002 to 40 Hz, were digitized and recorded on magnetic tape. The second three-component SQUID magnetometer was placed at one of the remote stations so that we could later perform reference magnetic MT processing for noise cancellation [*Gamble et al.*, 1979]. The other two remote stations consisted of a pair of orthogonal electrical dipoles and associated electronics. These remote telluric stations were used as quasi-tensor MT stations on the assumption that the magnetic field is spatially uniform over the distance between base and remote stations [*Hermance and Thayer*, 1976]. To check the assumption of magnetic field uniformity, one of the remote telluric stations became the base for the next set of measurements. In other cases, the reference magnetometer was located at a remote telluric station. Both procedures confirmed that the assumption of field uniformity holds.

Following the contractor's conventional data processing, all data were reprocessed by using both the remote magnetic and remote electric fields as reference fields. We found that both references worked well for calculating unbiased impedence estimates, but the impedance estimates calculated using the reference electric signals had larger statistical errors because of greater noise in the electric field.

Electromagnetic Surveys

Figure 4 shows the configuration of the EM-60 system, used for controlled-source EM soundings. A large magnetic moment ($>10^6$ mks) was created by impressing currents of

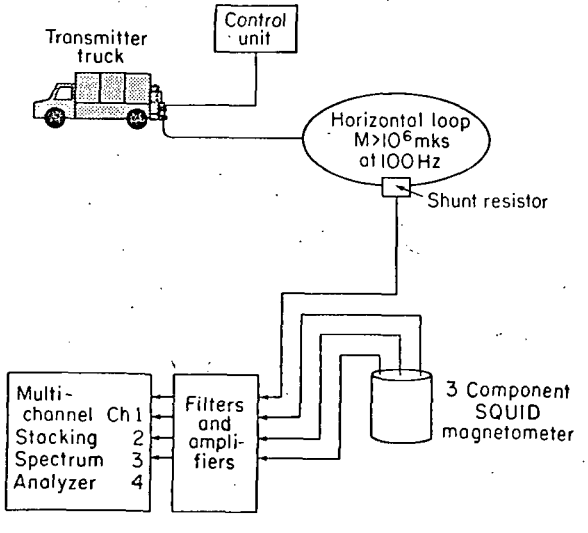

Fig. 4. The LBL controlled-source EM system (EM-60).

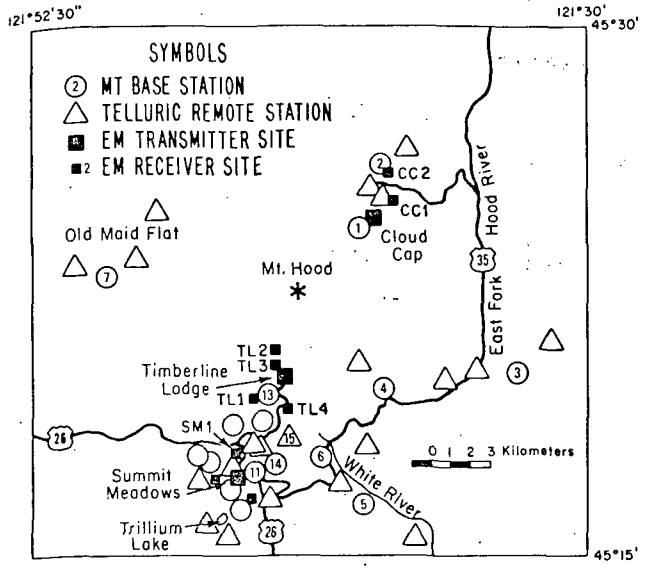

Fig. 5. Locations of MT and EM stations. The numbered stations are referred to in the text.

±65 A at ±150 V into a square loop consisting of three turns, 100 m on a side, of No. 6 welding cable. The frequency of the applied square wave current was remotely controlled and could be made to vary discretely between 10^{-3} and 10^{3} Hz. For this work, however, we were restricted to the frequency range 0.1–200 Hz because of large geomagnetic and atmospheric noise energy below and above this range, respectively.

At the receiver locations, magnetic field signals were detected by means of a three-component cryogenic (dc SQUID) magnetometer oriented to detect the vertical, radial, and tangential field components. Signals were amplified and band-pass filtered for anti-aliasing and signal-to-noise improvement, then were processed directly by means of a multichannel, microprocessor-controlled spectrum analyzer [*Morrison et al.*, 1978]. The spectrum analyzer stacked a specified number of cycles and computed and displayed an average 'raw' amplitude and phase relative to current phase in the loop. A hard-wire link between the spectrum analyzer and 0.01 ohm, 0.01% shunt resistor on the loop provided the phase reference. Spectral estimates were made at the fundamental and at higher odd harmonics, up to the seventh, as specified by the operator.

Data interpretation was accomplished by means of a one-dimensional inversion using an automatic Marquardt least squares approach [e.g., *Inman*, 1975]. The program fits amplitude/phase parameters of the field components normal to the plane of the loop (H_N and ϕ_N), radially outward from the loop (H_R and ϕ_R), and jointly fits polarization ellipse parameters (ellipticity and tilt angle). The tangential field, which should be absent over a layered earth or on a line perpendicular to a two-dimensional structure, was also monitored. Two-dimensional modeling, although possible, was not used for reasons of cost and the small number of stations.

Analysis of the EM data was complicated by the presence of cultural EM noise and sloping terrain. The noise required use of 60-Hz and 180-Hz notch filters whose effect on neighboring frequencies had to be carefully determined. More formidable was the rugged terrain, which resulted in a magnetic dipole vector inclined to the vertical. Because the resulting source is a combination of vertical and horizontal dipoles, it was necessary to correct the observed signals before an interpretation was made. As a first approximation, we mathematically rotated the vertical (H_N) and radial (H_R) components of the observed signals to find the fields normal to and in the plane of the transmitter loop. The criteria used to define these fields are that $H_N \rightarrow H_p$ and $H_R \rightarrow 0$ as $f \rightarrow 0$, where H_p is the calculated primary field at the magnetometer resulting from the transmitter dipole. One other approach successfully tested was to derive the ellipticity of the magnetic field polarization ellipse, which is independent of loop orientation, and to perform a one-dimensional interpretation on this information alone. Results from the ellipticity analysis compared rather well with results from a joint one-dimensional inversion of H_N and H_R amplitudes and phases. Because the ellipticity approach uses relative phase between H_N and H_R components rather than absolute phase, it also has the advantage of not requiring a phase reference link between transmitter and receiver.

RESULTS

Figure 5 shows the locations of MT base stations, remote telluric stations, and EM-60 transmitter and receiver stations. We concentrated stations in six main areas for various reasons: warm water emanations, geological interest, a nearby end-user of geothermal water, and above all, accessibility.

Cloud Cap

The Cloud Cap area lies on the NE flank of the mountain near a fairly recent (about 12,000 years old) eruptive center. The two MT and three remote telluric stations, all situated in

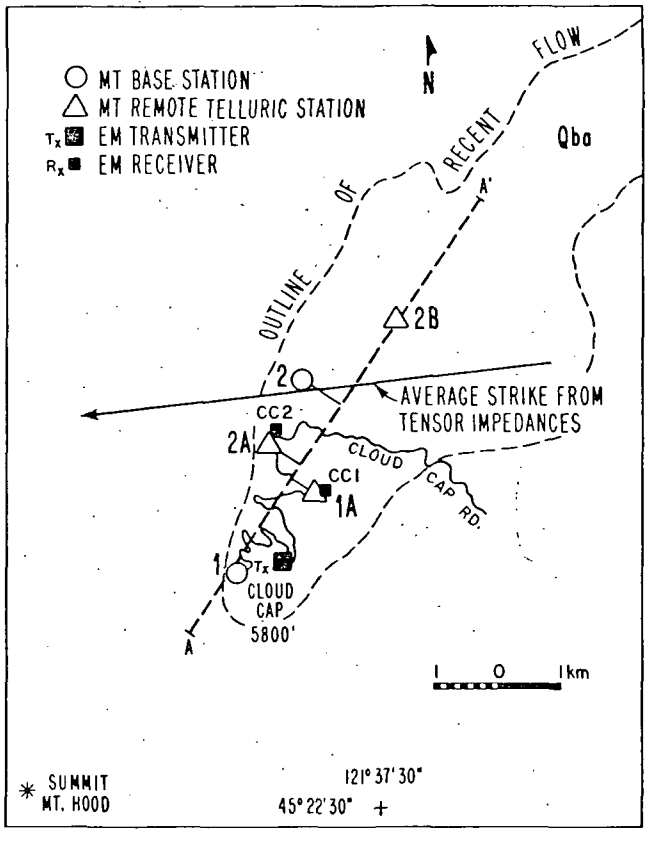

Fig. 6. Locations of MT and EM stations in the Cloud Cap area.

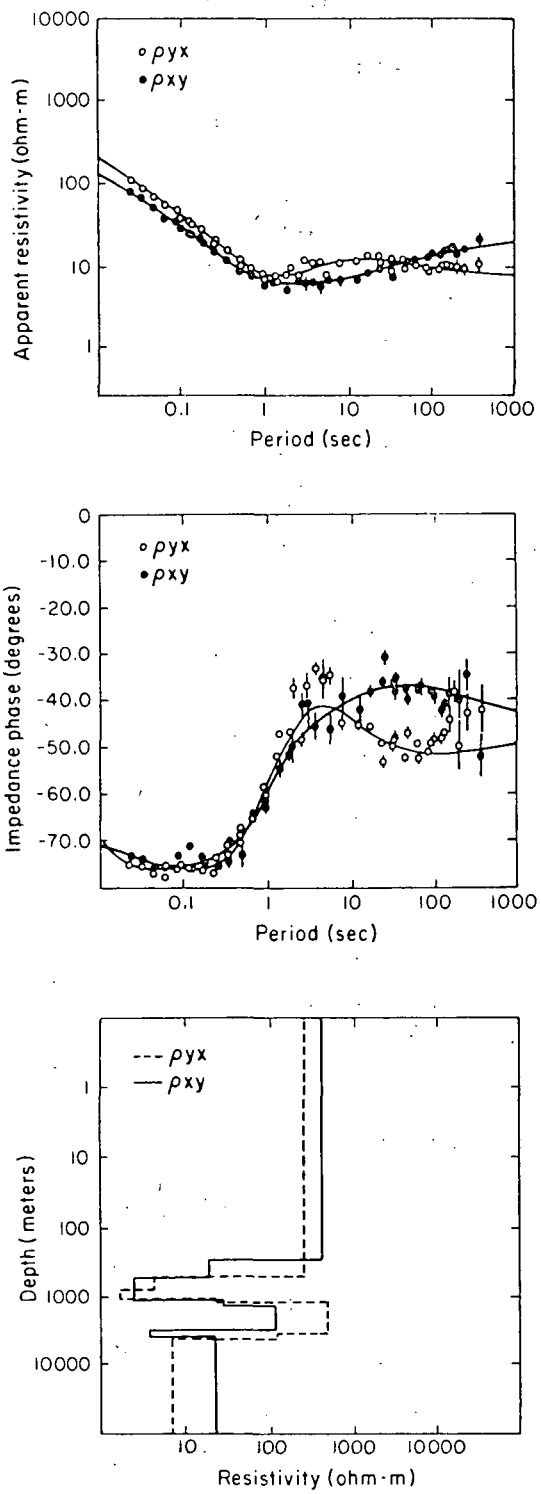

Fig. 7. Apparent resistivity amplitude and phase spectra of the ρ_{xy} and ρ_{yx} components observed at Cloud Cap, station 1. The layered-earth models are but two of many possible ones derived from an inversion of the amplitude and phase spectra.

the olivine basalt flow, extend from near the vent (elevation 1820 m) downhill a distance of 3 km (Figure 6). Two EM-60 soundings were made relative to a transmitter loop near the vent.

Using all impedance values of all five MT stations, the best average principal direction of the impedance tensor directions was found to be nearly east-west (S83°W). The tipper indicated a strike of N59°W. These results were

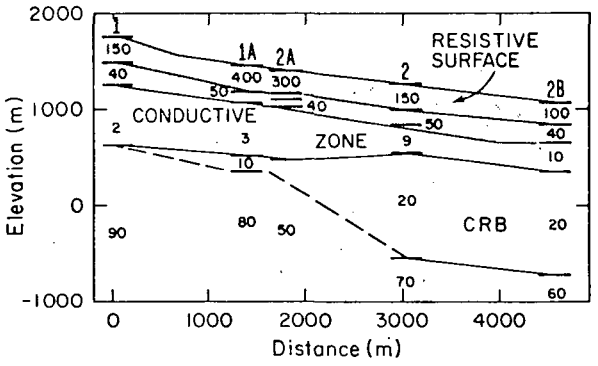

Fig. 8. One-dimensional interpretation of Cloud Cap line, electric field E-W (inferred electric field parallel-to-strike mode).

unexpected, since we had anticipated a northeasterly strike direction, i.e., radially outward from the summit or in the general direction of the successive volcanic flows and main erosional channels. After the average strike direction was determined, the apparent resistivities were calculated from the rotated impedances. These results were fitted to layered models according to a linearized, least squares inversion modeling scheme [*Jupp and Vozoff*, 1975], examples of which are shown in Figure 7 for station 1. The error bars are the 50% confidence limits using χ^2 distribution theory. A one-dimensional interpretation was justified on the basis of the similarity between ρ_{xy} and ρ_{yx} sounding curves, a similarity that exists mainly for the high-frequency (i.e., near-surface) regime. Because of the good quality of the high-frequency data at these stations, we overspecified the number of layers and obtained models with a relatively large number of near-surface layers.

To obtain a quasi two-dimensional model for the shallow region, we projected the results from all Cloud Cap stations into profile A-A', which is roughly radial to the cone, and obtained the sections shown in Figures 8 and 9. Both the ρ_{xy} section, identified as the electric field parallel-to-strike component, and the ρ_{yx} section, identified as the electric field perpendicular-to-strike component, show similar structure: (1) a continuous near-surface resistive layer, resistivities decreasing with depth and (2) an anomalously 'conductive zone' at a depth of 400–500 m. These features are more regular in the ρ_{xy} component (Figure 8), which shows that the conductive layer thickness decreases with distance away from the summit, while the layer resistivity increases from 2 to 10 ohm m. A somewhat similar result appears in the ρ_{yx} results (Figure 9). We also used a two-dimensional inverse

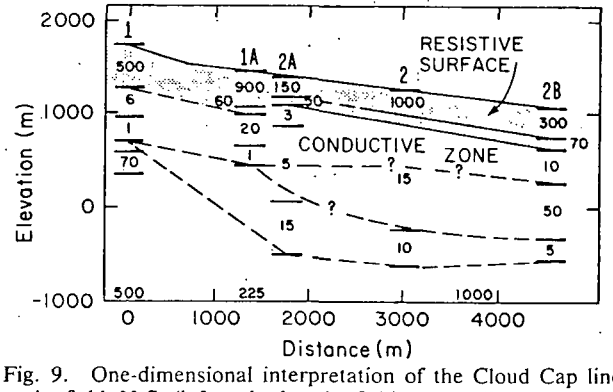

Fig. 9. One-dimensional interpretation of the Cloud Cap line, electric field N-S (inferred electric field perpendicular-to-strike mode).

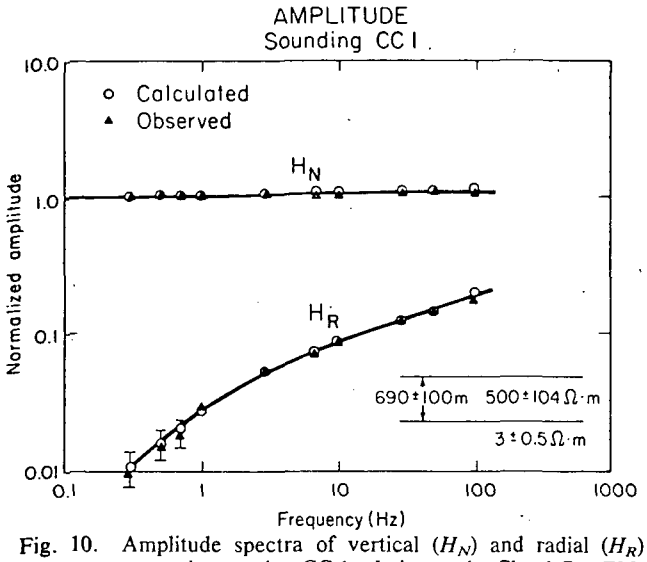

Fig. 10. Amplitude spectra of vertical (H_N) and radial (H_R) components at receiver station CC 1 relative to the Cloud Cap EM-60 transmitter loop.

modeling scheme [*Jupp and Vozoff*, 1977] to fit the data. Although we did not obtain a satisfactory model fitting all the data, the shallower section was very similar to that obtained from the one-dimensional inversions.

Beneath the conductive zone (i.e., below a depth of ~1 km) the results show less continuity, except between stations 2 and 2B, and it is difficult to draw conclusions regarding structure below −500 m in elevation. It has been questioned whether the change in character of the impedance and tipper functions between stations 1A/2A and 2 has actual geological significance or is merely a result of near-surface inhomogeneities. In an earlier report [*Goldstein et al.*, 1979] we speculated that a concealed E-W to NE-SW fault occurs between those stations.

On the basis of geophysical and drill hole data from the south flank (see next section), we have developed the following explanation for the shallow (≤2 km) geophysical results consistent with water geochemistry [*Wollenberg et al.*, 1979]. The resistive surface layer is a partially saturated zone in which cold meteoric waters flow through porous pyroclastic and jointed volcanic flows. The anomalously low resistivity beneath this layer corresponds to saturated Mount Hood volcanics containing warmer, possibly more saline, waters cooling progressively downslope as they mix with cold meteoric water. A possible heat source could be a still-hot Cloud Cap eruptive conduit or the main conduit beneath the summit.

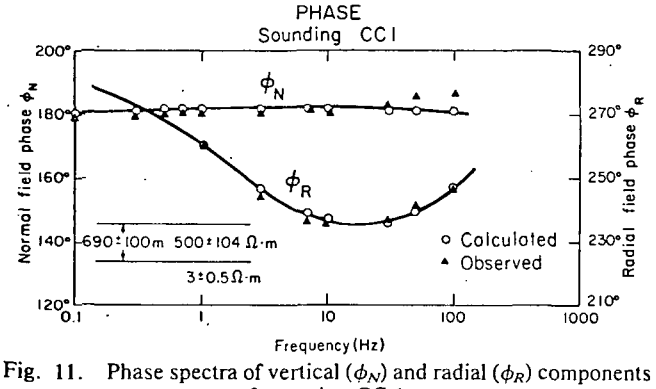

Fig. 11. Phase spectra of vertical (ϕ_N) and radial (ϕ_R) components for station CC 1.

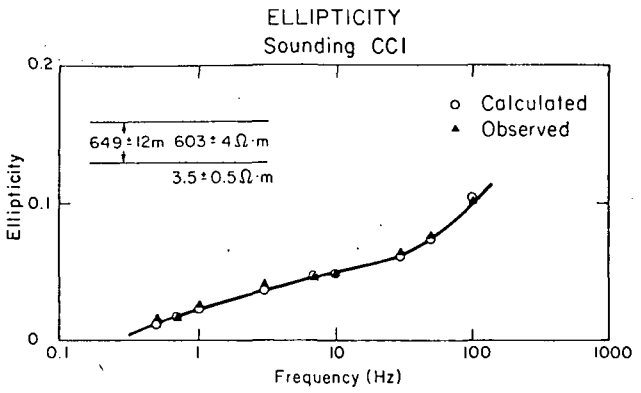

Fig. 12. Ellipticity spectrum for station CC 1 (see Figure 11).

The EM-60 sounding, for receiver CC 1 located 1 km from the transmitter loop, yielded data that were interpreted both through a joint inversion of the four amplitude and phase components and through an independent inversion of ellipticity only (Figures 10–12). Because of the small transmitter-receiver separation, the induced fields were unresponsive to the resistive zone below the conductive second layer; thus only a two-layer earth is discerned. It may also be seen that ellipicity inversion seemed to define first-layer parameters better than amplitude and phase, although both approaches gave the same low probable error for the second-layer resistivity. These errors are estimates for a parametric representation of the earth and are not accurate in terms of the real earth, which is considerably more complicated than our simple model of two layers and three parameters. The probable errors are geologically significant only to the extent that they indicate how closely we can fit the observed data to a simple layered model. The EM-60 sounding for receiver station CC 2 could not be fitted with low error to a layered earth, possibly because of the severe local relief between transmitter and receiver.

In general, EM sounding interpretations for station CC 1 are similar to the near-surface portion of the MT interpretations. The most obvious difference between the two is in the thickness of the resistive surface layer. This difference was noted at other sites at Mount Hood and will be discussed in the next section.

Timberline Lodge

Timberline Lodge is located at the 1820-m elevation on the relatively gently sloping south flank of Mount Hood. Because of continuing efforts by the lodge operator to find a source of hot water to heat the main lodge and a new day lodge, several MT and EM soundings were made in the area. An EM transmitter loop was laid out a short distance east of the main lodge, and four receiver stations were occupied at distances of 1–2 km from the transmitter. The most distant receiver (TL 2) was located at the top of the Miracle Mile chair lift (2425-m elevation), approximately 2 km north of Timberline Lodge. This was our closest approach to the summit.

Several MT soundings were attempted in the area, but because of noise, only station 13 provided enough data for an interpretation. However, this MT station and EM reciever station TL 4 are close to a geothermal test well later drilled at the base of the Pucci chair lift, 1 km south of the lodge.

Figure 13 shows the MT sounding results from station 13. The strong separation between apparent resistivities in the

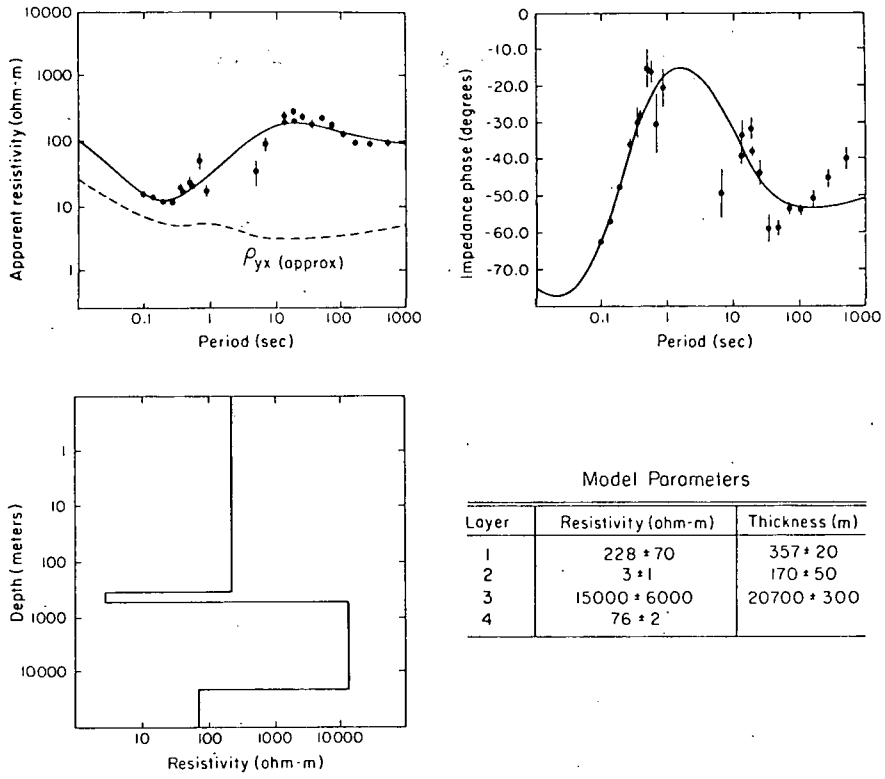

Model Parameters

Layer	Resistivity (ohm-m)	Thickness (m)
1	228 ± 70	357 ± 20
2	3 ± 1	170 ± 50
3	15000 ± 6000	20700 ± 300
4	76 ± 2	

Fig. 13. MT sounding curves for station 13 (Timberline Lodge) and the one-dimensional interpretation of the TE mode curve.

principal directions is an indication of two- and three-dimensional structures. Despite reference magnetic reprocessing, ρ_{xy} apparent resistivity values remain badly scattered in the range of 1–10 s, although the error statistics are immensely improved over the initial results. Because the electric field was strongly polarized in the area, we were unable to define a ρ_{yx} apparent resistivity sounding curve without large error. Consequently, the ρ_{yx} curve is drawn as a dashed line to indicate its approximate configuration.

Cognizant of the pitfalls of accepting a one-dimensional interpretation, we nevertheless show for the sake of comparison and discussion one such partial interpretation in Figure 13. Here, the same general near-surface layering is found as at Cloud Cap—a resistive surface layer, resistivity poorly resolved, underlain at a depth of approximately 350 m by a thin conductive zone. Of the many inversions made with constrained and unconstrained parameters, the one shown in Figure 13 for a joint inversion of apparent resistivity amplitudes and phases with no constraints yielded a fit as good as or better than others. The absence of high-frequency data points impairs our ability to resolve the resistivity of the surface layer, but this does not interfere with our resolution of the 3 ohm m second layer. Parameters derived for the third and fourth layers are probably in error, and no geological inferences should be drawn from them. In this regard, one should note the phase behavior at periods longer than, say, 30 s. The phase curves, as well as those shown in Figures 22 and 23, cannot be matched by any one-dimensional model, indicating that the deeper structure requires a multi-dimensional model.

Controlled-source EM sounding results relative to receivers located 1 km north and 1 km south of the Timberline

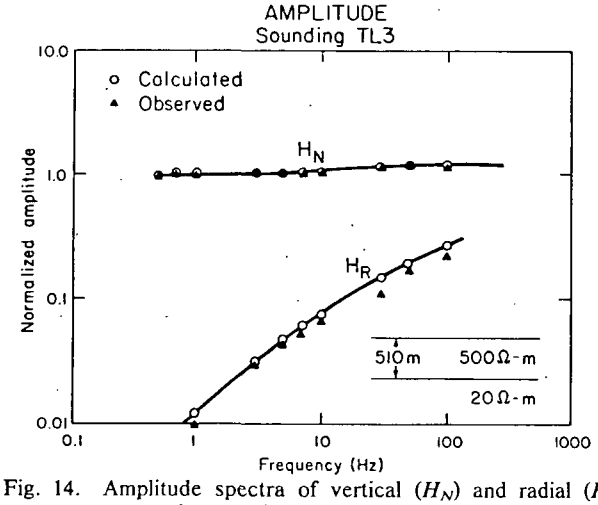

Fig. 14. Amplitude spectra of vertical (H_N) and radial (H_R) components at receiver station TL 3 relative to the Timberline Lodge EM-60 transmitter.

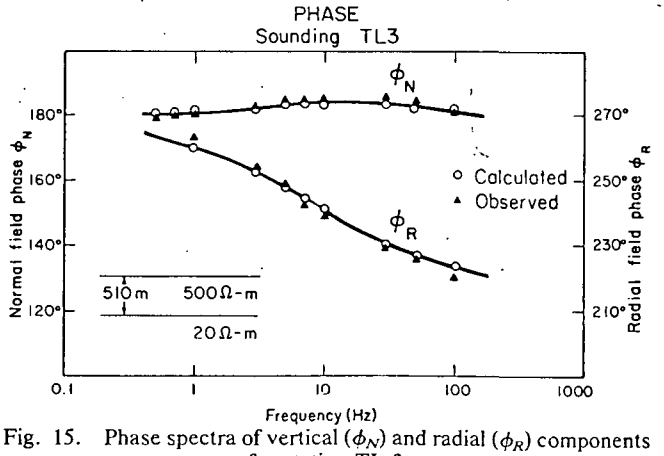

Fig. 15. Phase spectra of vertical (ϕ_N) and radial (ϕ_R) components for station TL 3.

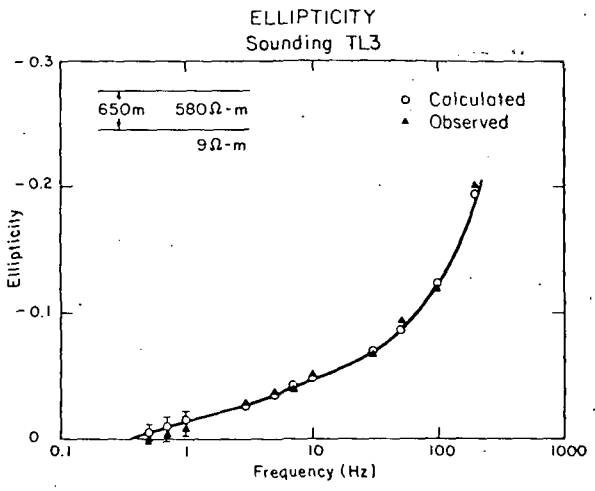

Fig. 16. Ellipticity spectrum for station TL 3.

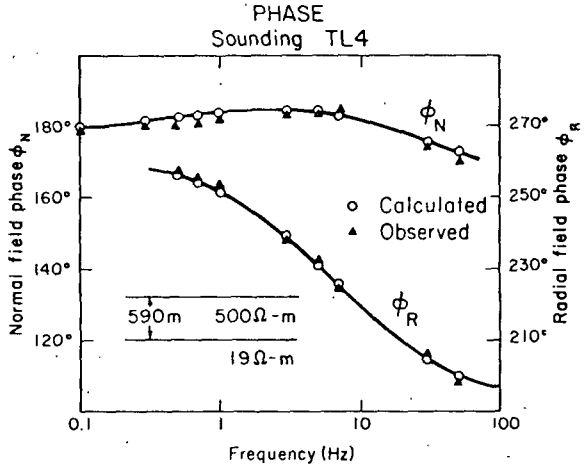

Fig. 18. Phase spectra of vertical (ϕ_N) and radial (ϕ_R) components for station TL 4.

transmitter (soundings TL 3 and TL 4, respectively) are shown in Figures 14–19. Since the results are not particularly sensitive to first-layer resistivity, we have constrained this parameter to 500 ohm m in the amplitude-phase inversion. Results show a layering similar to that found at the same elevation on the northeast flank (Cloud Cap). They also verify that the MT second-layer conductor is real and not an artifact of applying a one-dimensional inversion to two- and three-dimensional data. In contrast to the Cloud Cap area, it appears that the Timberline area has a thinner first layer and a less conductive second layer.

Comparing the Timberline MT and EM results, we see differences in the subsurface models that require some discussion and explanation. One notable difference is that the EM discerns a deeper and less conductive second layer. When the EM subsurface model is used in an MT forward calculation, the resulting curves differ significantly from those in Figure 13. While there may be several reasons for the differences in the models, one is that a one-dimensional inversion of MT data taken in complex areas is more susceptible to error than the one-dimensional inversion of the corresponding EM sounding because of the more focused nature of the dipole field. For example, we show in Figure 20 the error in the estimated depth to an embedded two-dimensional conductor that results when we apply a one-dimensional MT inversion. Curves $E_{\parallel}$ and $E_{\perp}$ are the calculated sounding curves for E field parallel-to-strike and perpendicular-to-strike, respectively. Performing the conventional one-dimensional inversion on $E_{\parallel}$ results in a three-layer model that fits the data very well. However, the conductor depth is underestimated by 34% in this example.

In the actual field case, the better accuracy of a one-dimensional inversion of the EM data seems to be verified by drill hole results. In 1980, the Pucci geothermal test hole (35/9E-7db) was drilled to a depth of 1213 m by the U.S. Geological Survey and DOE. The hole is located near MT station 13 and EM receiver station TL 4. Two weeks after drilling, the water level was 570 m below the surface, at which depth the temperatures were in the 40–50°C range and the bottomhole temperature appeared to be equilibrating at 70°–80°C (J. Robinson, personal communication, 1981). Because the top of the saturated zone conforms so closely to the interpreted EM conductor at 590 m (Figures 17 and 18), we feel reasonably confident that the second-layer conductor represents the saturated zone. The fact that the second

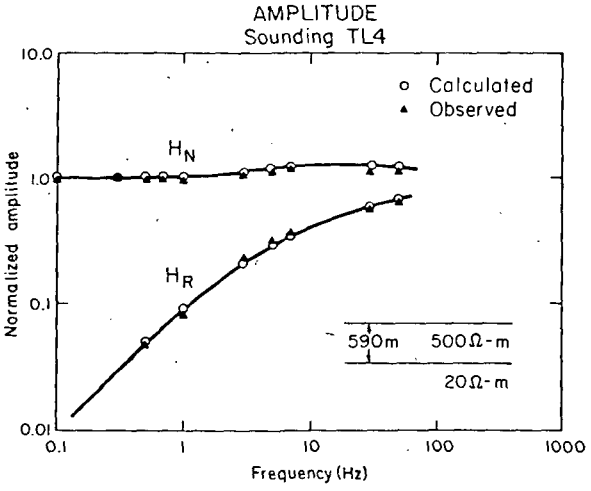

Fig. 17. Amplitude spectra of vertical (H_N) and radial (H_R) components at receiver station TL 4 relative to the Timberline Lodge EM-60 transmitter.

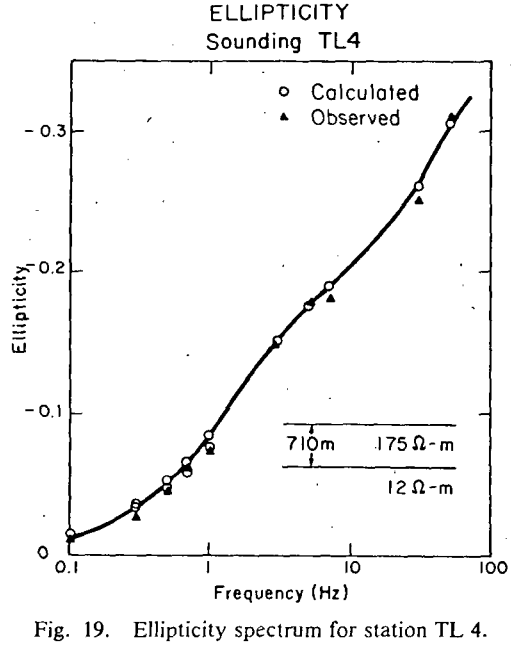

Fig. 19. Ellipticity spectrum for station TL 4.

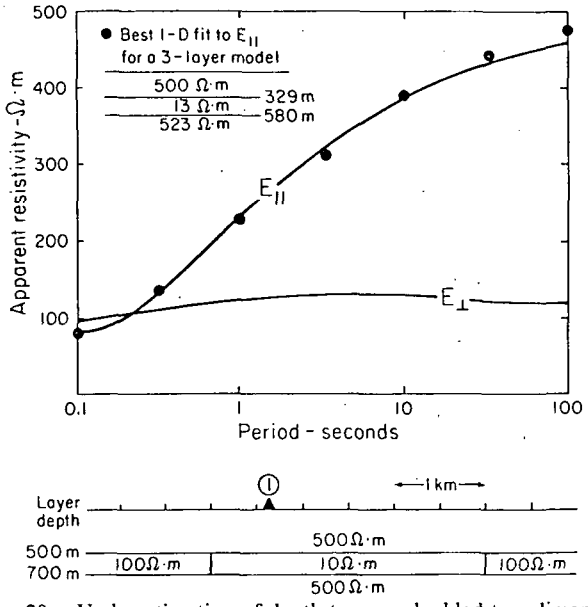

Fig. 20. Underestimation of depth to an embedded two-dimensional conductor using a one-dimensional inversion of the E field parallel-to-strike (E_{II}) component at station 1.

layer underlying the Cloud Cap area is 5 to 10 times more conductive than at Timberline Lodge may indicate that higher temperatures exist on the northeast flank of the volcano.

Summit Meadows

Summit Meadows (elevation 1106 m) lies approximately 10.5 km south of the summit and 1.5 km south of the Still Creek Campground, site of the warm waters known collectively as Swim Warm Springs. Because of this geothermal evidence, a number of MT stations and one EM-60 transmitter with three receiver sites were occupied in the NNE trending valley between Trillium Lake and Highway 26.

Three EM receivers were located north, west, and south of a transmitter loop laid out in Summit Meadows, but only the data from station SM 1, located 1.3 km north of the loop, are subject to simple interpretation (Figure 21). Although we obtain roughly the same type of resistivity section as higher on the flanks of the volcano, the surface layer is much less resistive in the meadows. The nearest MT station yielding good data is station 11 (Figure 22), and a one-dimensional inversion was made on the ρ_{xy} component. In this inversion we imposed a 50 ohm m constraint on the surface layer, as dictated by the EM results, and obtained a good fit to amplitude and phase data points. As at other stations, the MT gives a thinner first layer than the EM, but second-layer resistivities agree fairly well. Data from MT station 14, located 1 km east of station 11 on pre-Mount Hood volcanics, were interpreted on the basis of various constraints, including no constraints on layer parameters (Figure 23). At this site the conductive second layer is discerned at the same shallow depth but now appears as a thinner, more conductive zone.

Old Maid Flat

A cluster of one MT and three remote telluric MT stations were occupied in the Old Maid Flat area, 13.5 km west of the summit. This was the point closest to the road approach on the west flank and near the sites of the Old Maid Flat (OMF) 1 and OMF 7A geothermal wells drilled by Northwest Natural Gas and DOE to depths of approximately 1200 and 1838 m, respectively. Bottomhole temperatures were 82° and 112°C, respectively, but both holes are essentially dry at depth (J. Hook, personal communication, 1981).

Hood River

Two MT and four remote telluric stations were occupied in an approximate east-west line extending from Lookout Mountain on the east across the East Fork of the Hood River to the Hood River Meadows, a distance of 8 km. These stations were surveyed to determine whether MT could discern the postulated north-south normal fault following the river and the grabenlike structure related to crustal swelling and subsidence west of the river. A gradient hole was drilled to 352 m at Mount Hood Meadows (35/9E-3cca) by the U.S. Geological Survey and DOE in 1980. The bottomhole temperature was only 12°C, but the thermal gradient was 75°C km^{-1} in the lower part of the hole beneath a cold isothermal zone (J. Robinson, personal communication, 1981).

White River

Two MT and three remote telluric stations were occupied along an approximate north-south line in the White River area. These stations were surveyed to obtain more complete coverage on the south flank of the volcano.

Representation of Magnetotelluric Results Over the Survey Area

As a first step toward analyzing the lateral conductivity variations over an area, selected magnetotelluric parameters may be plotted in polar diagram form [*Reddy et al.*, 1977]. This procedure compresses and simplifies a great deal of information, thus allowing us to gain some geological insights as to local and regional structure. In this report, we show polar diagrams for both apparent resistivity (ρ_{xy}) and tipper magnitude (T_y). Figures 24–26 show these polar plots at each station for three bands—a high-frequency band between 10 and 40 Hz, a midband between 0.1 and 1.0 Hz, and a low-frequency band below 0.01 Hz.

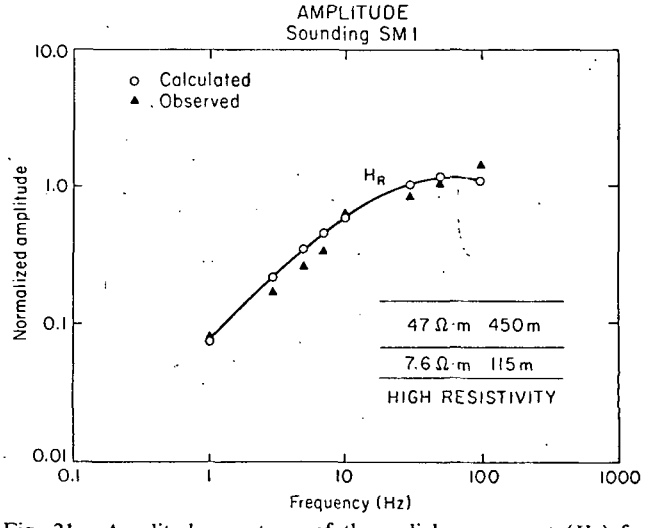

Fig. 21. Amplitude spectrum of the radial component (H_R) for station SM 1 in Summit Meadows.

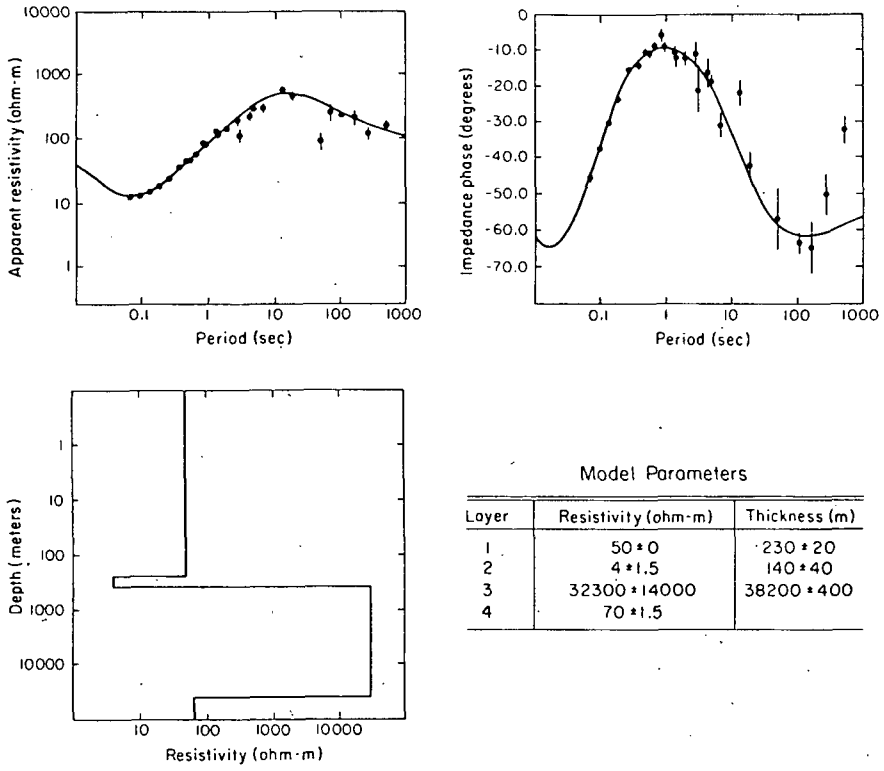

Model Parameters

Layer	Resistivity (ohm-m)	Thickness (m)
1	50 ± 0	230 ± 20
2	4 ± 1.5	140 ± 40
3	32300 ± 14000	38200 ± 400
4	70 ± 1.5	

Fig. 22. MT sounding curves at station 11, Summit Meadows, and the one-dimensional interpretation based on the TE mode.

The function ρ_{xy} (ϕ, ω), where ϕ is the azimuthal angle from north, was calculated from the off-diagonal term Z_{xy} (ω) of the impedance tensor. First, an analytical rotation of the Z_{xy} (ω) was performed over 360°, and these values were then averaged within selected frequency bands.

The size of the polar diagram is logarithmically related to apparent resistivity, and the maximum-minimum axes reveal the principal resistivity directions. A circular diagram is indicative of layered earth conditions, whereas a diagram constricted in one direction into a 'peanut' or 'figure 8' shape

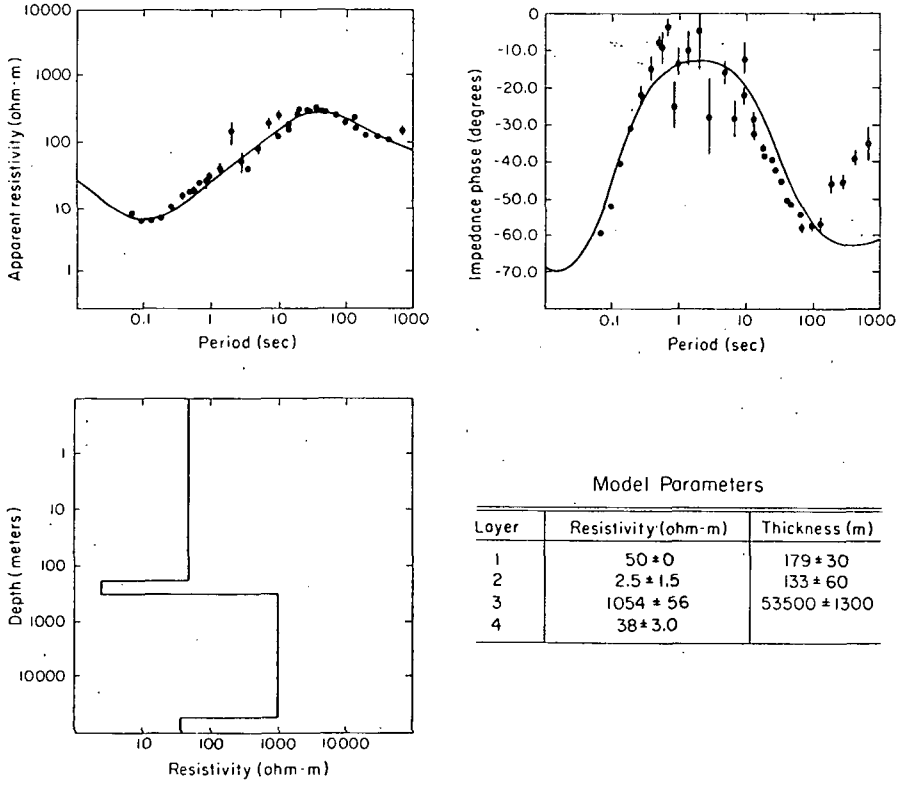

Model Parameters

Layer	Resistivity (ohm-m)	Thickness (m)
1	50 ± 0	179 ± 30
2	2.5 ± 1.5	133 ± 60
3	1054 ± 56	53500 ± 1300
4	38 ± 3.0	

Fig. 23. MT sounding curves at station 14, Summit Meadows, and the one-dimensional interpretation based on the TE mode.

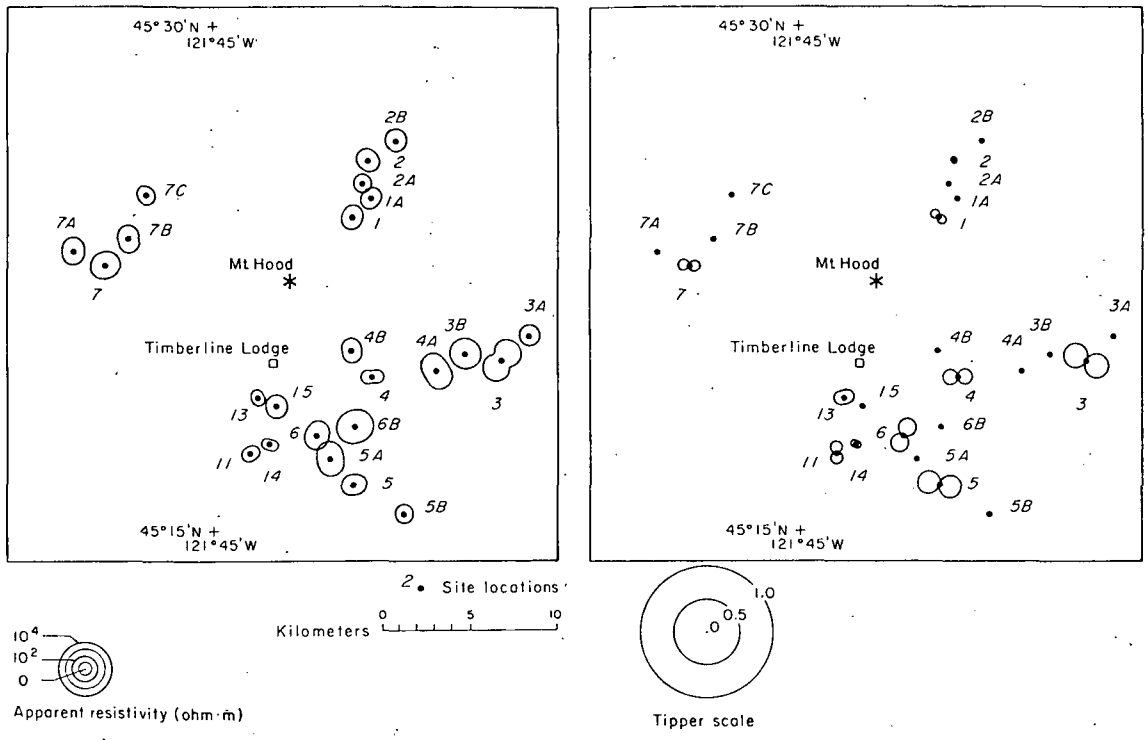

Fig. 24. Apparent resistivity and tipper polar diagrams, ρ_{xy} and T_y, averaged in the band above 10 Hz.

suggests resistivity anisotropy and current channeling in preferred directions. The high-frequency diagrams show the least nonuniformity, and the low-frequency diagrams show the greatest—indicating increasing structural complexity with depth. Several areas stand out as anomalous: (1) the low-resistivity zone previously discussed in reference to Cloud Cap, (2) a low-resistivity zone south of Timberline Lodge in the Summit Meadows–Swim Warm Springs area, where we see evidence for a north-south conductivity anomaly, and (3) the generally high resistivities and variable principal directions at stations 3 and 4, which span the Hood River (the river passes through station 3B). These plots also illustrate the horizontal distances over which large-scale resistivity changes occur.

On the scale of station clusters (~5 km), amplitudes and directions may remain fairly consistent (as at clusters 1 and

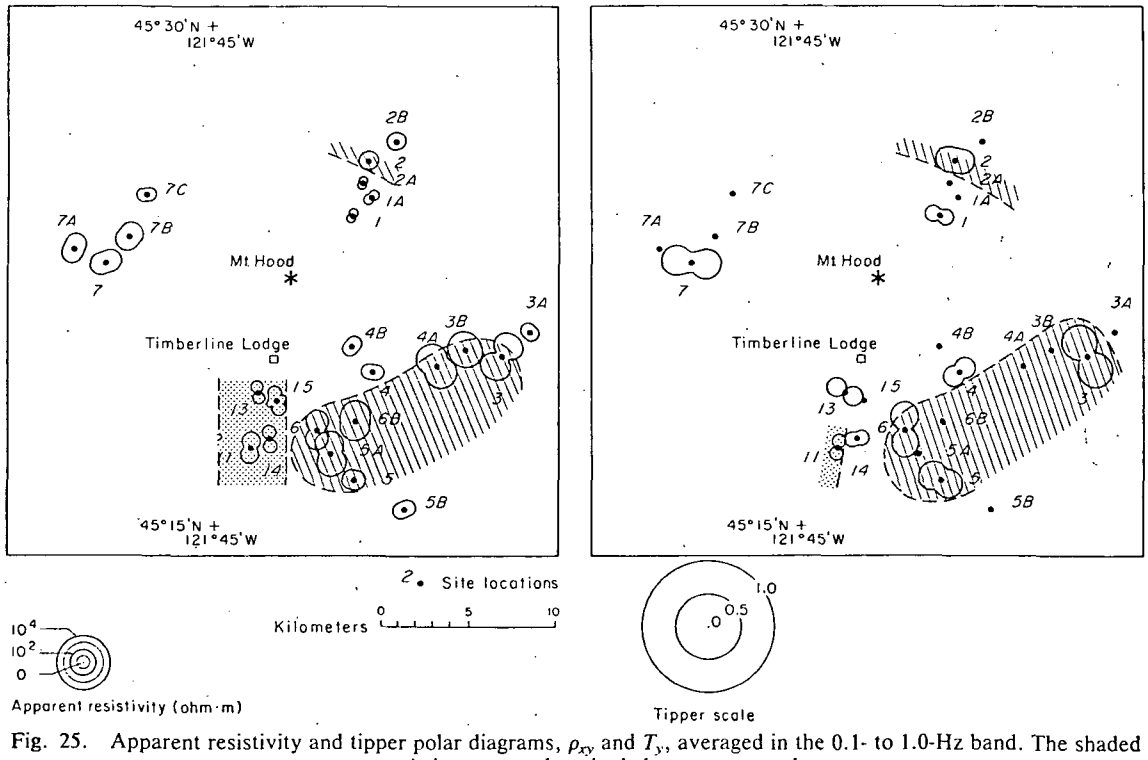

Fig. 25. Apparent resistivity and tipper polar diagrams, ρ_{xy} and T_y, averaged in the 0.1- to 1.0-Hz band. The shaded areas are resistive zones; the stippled areas are conductors.

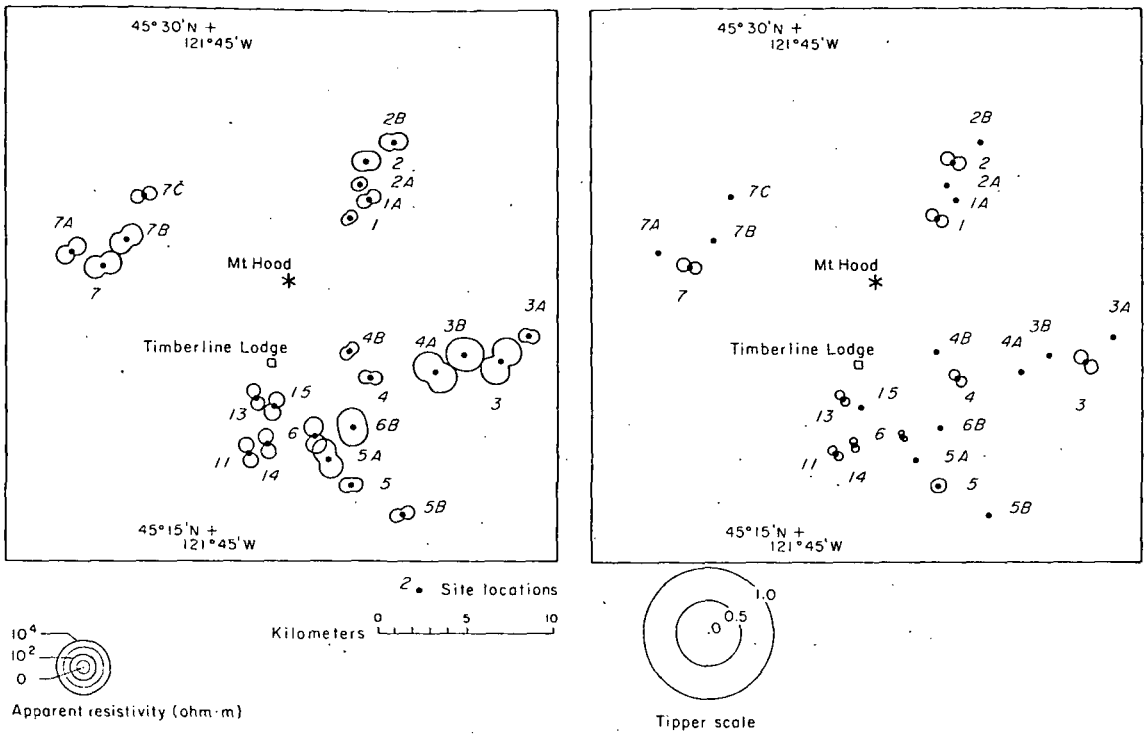

Fig. 26. Apparent resistivity and tipper polar diagrams, ρ_{xy} and T_y, averaged in the band below 0.01 Hz.

2, Cloud Cap) or change markedly by orders of magnitude and 90° over short distances, such as within cluster 3 (Hood River) and on the south side of the mountain (White River–Bennett Pass). A combination of local topography and geology seems to be the cause for the intracluster variability in several areas. For example, with the exception of the easternmost station 3C in cluster 3, the high apparent resistivities at all frequencies seem to be related to the older, pre–Mount Hood (Pliocene) volcanics at or near the surface east and west of the Hood River. Station 3C sits on Holocene basalt-andesite, close to the vent of an eruption of the same type and age as Cloud Cap. The station 3C apparent resistivity polar diagrams show higher conductivities and other characteristics similar to those at the Cloud Cap stations.

Complementary to the ρ_{xy} polar diagrams, we also show the corresponding tipper diagrams. These diagrams relate the amplitude ratio between the vertical and horizontal magnetic fields for a 360° rotation of the horizontal field. Theoretically, the tipper approaches zero over a layered or uniform earth and becomes large (but generally less than one) close to a vertical inhomogeneity. The direction of the maximum tipper is helpful in resolving the 90° ambiguity in the direction of geological strike from impedance information alone. In this paper, the tipper is plotted so that it is a maximum in a direction parallel to the strike of a two-dimensional structure.

At the low frequencies (Figure 26), both the apparent resistivity principal directions and tipper strikes indicate a NW-SE regional strike, similar to the conductor strike direction indicated by the 300-s-period transfer function derived by *Law et al.* [1980] from geomagnetic depth soundings across the Cascades in southern Washington. Tipper strikes are fairly consistent, but these directions show a curvature suggesting a transition to more resistive crust to the east and north of Mount Hood. Because of the limited number of stations, it is difficult to assign structural boundaries except in a few places. As discussed earlier and as shown in Figures 25 and 26, we have evidence for an east-west fault near station 2. Furthermore, the results on the south side of the volcano reveal some interesting structural features which seem to be best delineated in the midfrequency polar plots. One of the most striking features in Figure 26 is the large resistive zone (shaded area) lying at the base of the volcano between Barlow ridge (station 6) and the Hood River (station 3). Geologically, the surface consists of pre–Mount Hood Pliocene volcanics with local veneers of Recent river gravels and alluvium through which small exposures of lower Pliocene and small andesitic plugs are seen [*Wise*, 1968]. This area of resistive rock also correlates closely with a 4-mGal Bouguer gravity high [*Couch and Gemperle*, 1979]. It is therefore possible that the MT and gravity results outline an intrusive complex, possibly one similar in age and composition to the Still Creek and Laurel Hill stocks exposed south-southwest of the volcano.

West of this resistive block and south of Timberline Lodge and apparent resistivity diagrams suggest a north-south trending, moderately conductive zone, shown as the stippled area in Figure 25. The strike of the feature follows from calculated models which show that for stations on the conductive side of a two-dimensional inhomogeneity, the apparent resistivity will be a maximum in the direction of strike. However, except for station 11, a north-south, conductive zone is not well supported by tipper strikes at stations in the area. The large variability in tipper strikes in the high-frequency and midfrequency bands south of the summit probably represents a local three-dimensional feature.

CONCLUSIONS

Despite the obvious difficulties and limitations in performing EM surveys on the flanks of a Holocene stratovolcano,

MT and controlled-source EM surveys provided extremely interesting information. To resolve the deeper structure, a multi-dimensional interpretation is essential. However, one-dimensional modeling of MT and controlled-source EM soundings have provided information related to shallow stratigraphy and structure important to the understanding of the near-surface geology and geothermal resource potential.

On the northeast flank, MT data gave evidence for an E-W fault, possibly associated with a cauldron structure. Combined EM and MT soundings in the same area also served to trace a conductive 2–10 ohm m zone at a depth of 500–600 m that might represent a saturated zone of heated water. A similar zone was also discerned on the south flank, south of Timberline Lodge, where we also have information from a geothermal test well. Measurements in the well revealed a saturated zone of water in the 40°–50°C range at a depth of 570 m, close to the 590-m depth of a 20 ohm m conductor found by means of EM.

The south flank, where we have the highest concentration and number of MT stations, shows some interesting features. There seems to be a moderately conductive north-south grabenlike structure bounded on the east by resistive rocks, possibly a largely concealed, Pliocene intrusive complex coeval with the Laurel Hill and Still Creek intrusives exposed to the west.

The MT interpretation did not account for topography, admittedly on important considerations at some, if not most, of the stations occupied. Topography should induce an apparent two- or three-dimensional complexity different from, and in addition to, subsurface conditions. As a result of these complexities, one-dimensional MT interpretations generally underestimate the depth to the resistive basement beneath the station. On the other hand, a one-dimensional interpretation of the controlled-source EM data provides a more accurate measure of subsurface layering. However, we encountered other problems in using the EM system in nonflat terrain, e.g., the need to correct for (1) elevation differences between transmitter and reciever, (2) a dipole moment inclined to the frame of measurement, and (3) intervening terrain between transmitter and receiver. All but the last could be compensated for, and where intervening terrain was present, the data gave uninterpretable results.

Acknowledgments. This work was supported by the Assistant Secretary for Conservation and Renewable Energy, Office of Renewable Technology, Division of Geothermal and Hydropower Technologies of the U.S. Department of Energy under contract W-7405-ENG-48. Special thanks are due personnel of the State of Oregon, Department of Geology and Mineral Industries, the U.S. Forest Service, and the U.S. Geological Survey, who provided logistical help and scientific stimulation for those studies. In particular, we acknowledge the support of David Williams, U.S. Geological Survey; Donald Hull, Oregon Department of Geology and Mineral Industries; and John Geyer, U.S. Forest Service. The authors also wish to thank various colleagues who were involved in this program: Michael Hoversten and Mitchel Stark for data acquisition and data processing, and H. F. Morrison, Engineering Geosciences, University of California, Berkeley, for his continued support and guidance to the LBL Geothermal Program, and to this project in particular.

REFERENCES

Allen, J. E., The Cascade Range volcano-tectonic depression in Oregon, in *Transactions of the Lunar Geology Field Conference*, pp. 21–23, Oregon Department of Geology and Mineral Industries, Bend, 1966.

Bacon, C. R., Geology and geophysics of the Cascade Range, paper presented at the 51st Annual International Meeting, Soc. Expl. Geophys., Tulsa, Okla., 1981.

Beeson, M. H., and M. R. Moran, Stratigraphy and structure of the Columbia River basalt group in the Cascade Range, Oregon, Geothermal Resources Assessment of Mt. Hood, final report, pp. 5–77, Oreg. Dep. of Geol. and Mineral Ind., Bend, 1979.

Callaghan, E., Some features of the volcanic sequence in the Cascade Range in Oregon, *Eos Trans. AGU*, 243–249, 1933.

Couch, R., and M. Gemperle, Gravity measurements in the area of Mt. Hood, Oregon, Geothermal Resources Assessment of Mount Hood, final report, pp. 137–187, Oreg. Dep. of Geol. and Mineral Ind., Bend, 1979.

Crandell, D. R., Recent eruptive history of Mount Hood, Oregon, and potential hazards from future eruptions, *U.S. Geol. Surv. Bull., 1492*, 1980.

Crandell, D. R., and M. Rubin, Late glacial and post-glacial eruptions at Mt. Hood, Oregon, *Geol. Soc. Am. Abstr. Programs*, *9*(4), 406, 1977.

Folsom, M. M., Volcanic eruptions: The pioneers' attitudes on the Pacific Coast from 1800 to 1875, *Ore Bin*, *32*(4), 61–71, 1970.

Gamble, T. D., W. M. Goubau, and J. Clarke, Magnetotellurics with a remote reference, *Geophysics*, *44*, 53–68, 1979.

Goldstein, N. E., and E. Mozley, A telluric-magnetotelluric survey at Mt. Hood, Oregon—A preliminary study, *Rep. LBL-7050*, Lawrence Berkeley Lab., Berkeley, Calif., 1978.

Goldstein, N. E., E. Mozley, T. D. Gamble, and H. F. Morrison, Magnetotelluric investigations at Mt. Hood, Oregon, *Trans. Geotherm. Resour. Counc.*, *2*, 219–221, 1978.

Goldstein, N. E., M. Wilt, M. Stark, E. Mozley, and H. F. Morrison, Magnetotelluric and controlled-source electromagnetic studies at Mt. Hood, Oregon, *Rep. LBL-9776*, Lawrence Berkeley Lab., Berkeley, Calif., 1979.

Hermance, J. F., and R. E. Thayer, The telluric-magnetotelluric method, *Geophysics*, *40*, 664–668, 1976.

Inman, J. R., Resistivity inversion with ridge regression, *Geophysics*, *38*, 798–817, 1975.

Jupp, D. L. B., and K. Vozoff, Stable iterative methods for the inversion of geophysical data, *Geophys. J. R. Astron. Soc.*, *42*, 957–976, 1975.

Jupp, D. L. B., and K. Vozoff, Two-dimensional magnetotelluric inversion, *Geophys. J. R. Astron. Soc.*, *50*, 333–352, 1977.

Law, L. K., D. R. Auld, and J. R. Booker, A geomagnetic variation anomaly coincident with the Cascade Volcanic Belt, *J. Geophys. Res.*, *85*, 5297–5302, 1980.

Morrison, H. F., N. E. Goldstein, M. Hoversten, G. Oppliger, and C. Riveros, Description, field test and data analysis of a controlled-source EM system (EM-60), *Rep. LBL-7088*, Lawrence Berkeley Lab., Berkeley, Calif., 1978.

Reddy, I. K., D. Rankin, and R. J. Phillips, Three-dimensional modeling in magnetotelluric and magnetic variational sounding, *Geophys. J. R. Astron. Soc.*, *51*, 313–325, 1977.

Stanley, W. D., A regional magnetotelluric survey of the Cascade Mountain region, *U.S. Geol. Surv. Open File Rep., 82–126*, 1982.

Thayer, T. P., Petrology of the later Tertiary and Quaternary rocks of the north-central Cascade Mountains in Oregon, with notes on similar rocks in Nevada, *Geol. Soc. Am Bull.*, *48*, 1611–1652, 1937.

Wilt, M., N. E. Goldstein, M. Hoversten, and H. F. Morrison, Controlled-source EM experiment at Mt. Hood, Oregon, *Trans., Geotherm. Resour. Counc.*, *3*, 789–792, 1979.

Wise, W. S., Mount Hood area, Andesite Conference Guidebook, *Bull. Oreg. Dep. Geol. Miner. Ind.*, *62*, 81–98, 1968.

Wollenberg, H. A., R. E. Bowen, A. R. Bowman, and B. Strisower, Geochemical studies of rocks, water, and gases at Mt. Hood, Oregon, *Rep. LBL-7092*, Lawrence Berkeley Lab., Berkeley, Calif., 1979.

(Received March 25, 1981;
revised September 11, 1981;
accepted December 11, 1981.)